

The vibrational structure of benzene adsorbed on Si(001)

Markus Stauer, Uwe Birkenheuer, Thomas Belling, Folke Nörtemann,
and Notker Rösch

*Institut für Physikalische und Theoretische Chemie, Technische Universität München, 85747 Garching,
Germany*

Wolf Widdra, Krassimir L. Kostov, Thomas Moritz, and Dietrich Menzel

Physik Department E20, Technische Universität München, 85747 Garching, Germany

(Received 31 August 1999; accepted 4 November 1999)

High resolution electron energy loss spectroscopy (HREELS) measurements and density functional model cluster calculations are presented to clarify the vibrational structure of the adsorption system $C_6H_6/Si(001)$. All vibrational modes of the adsorption complex, which previously was identified to exhibit a cyclohexadiene-like structure, have been calculated and characterized according to the motion of the different atoms of the adsorption complex. Special emphasis is placed on the low-frequency modes. The coupling between the adsorbate and the substrate modes is analyzed with the help of a model that represents various limiting situations. Different coupling variants are found to apply to different collective modes of the adsorbate. The A_1 and B_1 modes can be described rather well by a model that only encompasses the adsorbate and the Si dimer underneath; for the A_2 and B_2 modes a frozen substrate description of the adsorption complex is more appropriate.

© 2000 American Institute of Physics. [S0021-9606(00)70505-8]

I. INTRODUCTION

The adsorption of benzene on the (2×1) dimer reconstructed Si(001) surface has been the subject of several experimental and computational investigations. Among the earliest is an experimental study¹ based on thermal desorption spectroscopy (TDS), low energy electron diffraction (LEED), and high resolution electron energy loss spectroscopy (HREELS). Semiempirical MINDO (modified intermediate neglect of differential overlap) and PM3 [parametric model 3 of the MNDO (modified neglect of diatomic overlap) approach] calculations on this adsorption system followed,^{2,3} but it was only recently that in a combined experimental and theoretical study,^{4,5} the structure of the adsorption complex could unambiguously be assigned by comparing angle-resolved ultraviolet photoemission spectroscopy (ARUPS) and HREELS data with results of “first principles” density functional (DF) calculations for various structure models. Benzene is di- σ bound to a single Si surface dimer forming a C_{2v} -symmetric adsorption complex in which carbon atoms in 1,4 (para) positions form Si-C bonds and the remaining parts of the benzene skeleton are bent upwards in “butterfly” fashion (Fig. 1).

In the meantime new scanning tunneling microscopy (STM) images for $C_6H_6/Si(001)$ have been recorded by various groups^{6–9} and partially complemented by semiempirical AM1 calculations.^{7,8} In Refs. 6–8 a symmetric but metastable adsorption complex is identified which is attributed to the butterfly complex just mentioned. These studies associated the most stable configuration of benzene on Si(001) with a tilted structure, either bound to a single dimer as proposed previously,^{1,6} or four-fold bound to two neighboring surface dimers as favored by some of the semiempirical calculations.^{2,7,8} Thus, the discussion on the structure of the adsorption complex $C_6H_6/Si(001)-(2 \times 1)$ has been reopened. No asymmetric STM patterns due to tilted benzene mol-

ecules on Si(001) are reported in Ref. 9. Hence, the nature of the two adsorption species remains unclear. Moreover, no hints for a configuration of benzene on Si(001) that is more stable than the butterfly structure have ever been found in any of our HREELS experiments (see below). In addition, we would like to point out that we, too, had carried out semiempirical [MNDO/d (MNDO with d functions)] calculations,⁵ but had rejected the results concerning the energetic preference of the various adsorption complexes since they turned out to be at variance with those of more reliable “first principles” DF calculations (with deviations of the binding energies in the order of a few eV). It seems that semiempirical calculations tend to systematically overestimate the strength of the Si-C bonds in this particular adsorption system, and thus spuriously favor four-fold coordinated equilibrium structures. Moreover, preliminary gradient corrected DF cluster model calculations¹⁰ indicate that tilted equilibrium geometries are by about 0.5 eV less stable than the butterfly structure.

Here we will focus on the vibrational properties of the 1,4-cyclohexadiene-like butterfly adsorption complex found previously.^{4,5} In this C_{2v} -symmetric equilibrium configuration of benzene adsorbed on Si(001) the characteristic aromatic π system of free benzene is destroyed and the two carbon centers which bind to the Si surface dimer change their hybridization to sp^3 . The four remaining carbon atoms bent upward while keeping their original sp^2 hybridization such that a double bond remains in each of the two parts of the distorted benzene ring. These double bonds give rise to a vibrational frequency at about 1600 cm^{-1} in the calculated spectrum of the butterfly structure model. The presence of this mode in the experimental HREELS data available at that time¹ was one of the arguments favoring the butterfly structure over the other C_{2v} -symmetric structure considered.⁵ That previous analysis of the vibrational properties of the

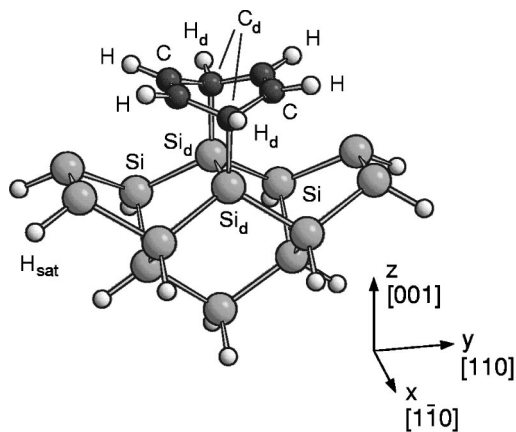


FIG. 1. Butterfly cluster model of C_6H_6 adsorbed on Si(001).

adsorption complex, however, was limited due to lack of data. Comparison between experimental and theoretical results was based on a HREELS study¹ which, from the present point of view, exhibits a rather poor resolution and, in addition, only comprises vibrational features above 500 cm^{-1} . Therefore, a comparative discussion of the soft vibrational modes and, in particular, of the coupling of the adsorbate modes to the substrate was not feasible. Moreover, no systematic analysis of the nonsymmetric modes was performed, although all modes had been calculated with a semiempirical method. The limited experimental resolution and the apparently large uncertainty inherent to the semiempirical approach for benzene on Si(001) did not allow an assignment of the manifold of nonsymmetric modes.

Stimulated by new HREELS measurements on the adsorption system $C_6H_6/Si(001)$ with a significantly improved resolution, we decided to perform new “first principles” DF calculations which now comprise all vibrational modes. Moreover, in view of the extended experimentally accessible frequency range it seems worthwhile to analyze also the low-lying vibrational modes which involve both adsorbate and substrate components. The main emphasis of this paper will be on the theoretical aspects. Detailed experimental results will be presented elsewhere.¹¹

II. EXPERIMENTAL DETAILS

The experiments were performed in a two-chamber ultrahigh vacuum system which has been described previously.¹² Briefly, it is equipped with standard four-grid LEED optics, quadrupole mass spectrometer, Kelvin probe, Ar^+ -ion sputter gun, different dosing facilities, x-ray source and a hemispherical analyzer for XPS (x-ray photoelectron spectroscopy). Separated by a gate valve an HREEL spectrometer (Delta 05, VSI) is available. With it, resolutions better than 8 cm^{-1} (1 meV) at count rates of $6\text{--}10 \times 10^5\text{ s}^{-1}$ are routinely achieved on metal surfaces. The experiments were performed on a vicinal Si(001) crystal (miscut 5° towards the [110] direction, phosphorus doped, $8\text{--}12\ \Omega\text{ cm}$) to achieve (2×1) single-domain terraces. Sample treatment and details of the sample mounting have been described previously.⁴ For the data shown here, gas dosing and data acquisition were performed at 90 K. The thermal exci-

tation of low-energy plasmons at this temperature leads to a broadening of the quasielastic peak and limits the experimental resolution to 27 cm^{-1} at our doping level.

III. COMPUTATIONAL DETAILS

A. General

The calculations were performed with PARAGAUSS,^{13,14} a new parallel implementation of the linear combination of Gaussian-type orbitals density-functional (LCGTO-DF) method.^{15,16} We adopted the basis sets from our first study on $C_6H_6/Si(001)$.⁵ The exchange-correlation contributions were obtained by numerical integration over overlapping atomic grids^{17,18} which are improved with respect to those used previously.⁵ The local density approximation (LDA) of Vosko, Wilk, and Nussair¹⁹ together with the gradient corrections proposed by Becke²⁰ and Perdew^{21,22} (generalized gradient approximation, GGA) was applied during the SCF (self-consistent field) procedure and for calculating the analytical energy gradients. In line with previous findings⁵ all calculations were performed in spin-restricted fashion.

The Si(001) surface was represented by the cluster model used before for the butterfly structure⁵ (see Fig. 1; dangling bonds of Si centers were saturated by hydrogen atoms). The positions of the Si atoms of the surface dimer below the benzene molecule, i.e., the dimer which is directly involved in the covalent Si–C bonds, were included in the geometry optimization whereas the positions of the remaining substrate atoms were kept fixed at their bulk-terminated values. The equilibrium structure of the cluster model $C_6H_6Si_{13}H_{12}$ was reoptimized to take into account effects of the improved integration grid. However, structural changes with respect to the previous results⁵ were found to be negligible.

To analyze the effect of the Si surface on the vibrational normal modes, a molecular model $C_6H_6Si_2H_4$ was considered as well. This molecular system was subject to a full geometry optimization within C_{2v} symmetry constraints.

B. Calculation of vibrational normal modes

All vibrational frequencies and normal modes were calculated in harmonic approximation by diagonalizing the mass-weighted force constant matrix which was obtained by finite differences of energy gradients. To this end all internal degrees of freedom, i.e., bond length, angles, and dihedral angles, were displaced by $\pm 0.02\text{ a.u.}$ and $\pm 0.02\text{ rad}$, respectively, from their equilibrium values, breaking C_{2v} symmetry. For computational convenience these displacements were chosen according to the four irreducible representations of the point group C_{2v} and the normal modes for each irreducible representation were calculated separately. In doing so the remaining symmetry was exploited (C_{2v} for A_1 , C_2 for A_2 , and C_s for B_1 and B_2). To test the numerical accuracy of this approach the vibrational frequencies of a free benzene molecule were calculated and found to differ by at most 2 cm^{-1} from the results obtained by a reference calculation carried without any symmetry constraints. The surface dimer that participates in the adsorbate–substrate bond was included in the full vibrational analysis, the rest of the

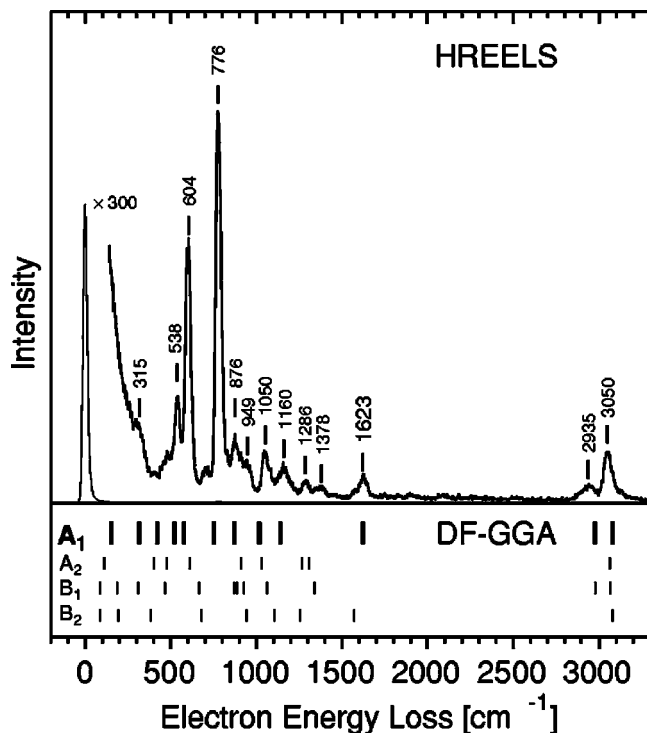


FIG. 2. Comparison of the HREELS data for $C_6H_6/Si(001)$ with the calculated normal frequencies of the model cluster $C_6H_6Si_{13}H_{12}$. The calculated frequencies are indicated by vertical bars, separated according to the four irreducible representations of the symmetry group C_{2v} .

substrate was kept fixed. The frequencies of the totally symmetric modes essentially coincide with the previous values;⁵ frequencies deviate at most by 26 cm^{-1} . The main reason for switching to the improved grid was to ensure the same high integration quality for both the symmetric and the nonsymmetric modes.

IV. RESULTS AND DISCUSSION

The experimental spectra for $C_6H_6/Si(001)$ and the calculated vibrational frequencies for the model cluster $C_6H_6Si_{13}H_{12}$, ordered according to the symmetry character of the individual modes, are presented in Fig. 2. The HREELS data are shown for benzene adsorption at 90 K and subsequent desorption of the physisorbed benzene multilayers. The spectrum was recorded with a primary energy of 4 eV in specular scattering geometry. Here the experimental resolution is enhanced by a factor 2.5 compared to a previous study¹ and thus several new features can be identified. Annealing the saturated monolayer to 350 K, i.e., to just below the onset of thermal desorption, does not alter the vibrational spectrum. This clearly demonstrates the thermal stability of the saturated layer. Any conversion from a metastable to a stable structure as observed at room temperature by STM (Refs. 6–8) can be ruled out.

The results of the assignment of all calculated vibrational modes based on an analysis of the eigenvectors of the mass-weighted force constant matrix are presented in Table I. Actually most of the vibrational modes, especially those with frequencies between 400 and 900 cm^{-1} , represent mixtures of simple internal modes such as bond stretching and

single bond bending or frustrated motions. In those cases the description in Table I is restricted to the most dominant features (in the order of importance).

The vibrational spectrum of $C_6H_6/Si(001)$ can roughly be grouped into the following energy regions. Below the C–H stretching frequencies at about $3000\text{--}3100\text{ cm}^{-1}$, which mark the high-energy end of the spectrum, the stretching modes of the C=C double bonds between the sp^2 hybridized carbon atoms show up around 1600 cm^{-1} . The in-plane bending modes of the C–H groups appear between 1350 and 1100 cm^{-1} . From 1050 down to 650 cm^{-1} the corresponding out-of-plane modes can be observed. In this frequency range also deformation modes of the benzene skeleton are present. In part, these latter modes also include contributions from motions of the substrate atoms. Finally, at the low-energy end of the spectrum, the collective motions (frustrated rotations or translations) of the entire benzene molecule and of the surface dimer underneath appear. In the adsorption system $C_6H_6/Si(001)\text{--}(2\times 1)$ there exists a second kind of dimer, the one not having a benzene molecule bound to it (Fig. 1). Yet, to avoid overloading the terminology, the former type of dimer, in which we are mainly interested here, will simply be referred to as *the* surface dimer.

Within the various frequency regions the shape of the normal modes is predominately determined by symmetry. The normal modes consist of symmetry-adapted linear combinations of internal modes according to the irreducible representations of the C_{2v} symmetry group of the adsorption complex. Sometimes normal modes consisting of the same type of internal modes, but belonging to different irreducible representations, exhibit quite different frequencies, as illustrated by the out-of-plane bending modes of the sp^2 C–H groups. While in the modes of A_1 and B_2 symmetry [Figs. 3(j,k)] the C–H groups belonging to the same C=C double bond are moving in phase, in the corresponding A_2 and B_1 modes the hydrogen atoms are bending up and down out-of-phase [Figs. 3(i,h)]. Thus, in the latter two modes the bending of the C–H groups is accompanied by a torsion of the C=C π bond, resulting in larger force constants and, in turn, in significantly higher frequencies.

After this overview we now turn to a more detailed analysis of some of the individual normal modes. For convenience this discussion will treat the totally symmetric and the nonsymmetric modes separately.

A. The totally symmetric modes

As the totally symmetric normal modes of the adsorption complex $C_6H_6/Si(001)$ have already been discussed previously,⁵ we shall focus here on the new aspects, i.e., on the modes with low frequencies.

The normal mode related to the lowest frequency (calculated at 154 cm^{-1} , experimentally not observed) consists of a collective in-phase motion perpendicular to the surface that involves the entire benzene molecule and the surface dimer (see Table I); stretching of the benzene-dimer bonds contributes to a small extent only. The normal mode which has to be assigned to the benzene-dimer stretching, the frustrated translation T_z of benzene, exhibits a frequency of 523 cm^{-1} ; experimentally this mode is found at 538 cm^{-1} .

TABLE I. Vibrational frequencies $\nu(\text{C}_6\text{H}_6)$ of $\text{C}_6\text{H}_6/\text{Si}(001)$ as obtained from the model cluster $\text{C}_6\text{H}_6\text{Si}_3\text{H}_{12}$ and the corresponding frequencies $\nu(\text{C}_6\text{D}_6)$ of the deuterated complex (in cm^{-1}). Also shown are the relative contributions $E_{\text{kin}}(\text{H})$ and $E_{\text{kin}}(\text{D})$ of benzene, hydrogen, and deuterium atoms, respectively, to the kinetic energy of the normal modes (in percent). The last column provides a characterization of the calculated non-deuterated normal modes. Major contributions are given first. For the labeling of the atoms and the orientation of the coordinate axes, see Fig. 1.

$\nu(\text{C}_6\text{H}_6)$	$\nu(\text{C}_6\text{D}_6)$	$E_{\text{kin}}(\text{H})$	$E_{\text{kin}}(\text{D})$	Assignment
<i>A₁</i> modes				
154	148	7	9	T_z of the $\text{C}_6\text{H}_6\text{-Si}_2$ moiety
318	285	21	44	butterfly bending + T_2 of $\text{C}_6\text{H}_6\text{-Si}_2$ (C_d motions in phase)
419	407	6	11	dimer stretching
523	486	17	20	$\text{Si}_d\text{-C}_d$ stretching + butterfly bending (C_d motion in phase)
577	542	19	19	$\angle(\text{C}, C_d, \text{C})$ bending
755	634	51	59	collective out-of-plane C-H and $C_d\text{-H}_d$ bending (in phase)
870	835	16	22	benzene breathing
1016	747	80	63	isolated out-of-plane $C_d\text{-H}_d$ bending
1140	835	92	74	in-plane C-H bending
1623	1583	7	10	C=C stretching
2978	2193	92	83	$C_d\text{-H}_d$ stretching
3081	2291	91	78	C-H stretching
<i>A₂</i> modes				
109	99	21	34	R_z of C_6H_6
402	390	3	24	R_z of the dimer
474	431	20	28	R_z of the C=C bonds around their centers
608	575	10	25	benzene carbon ring (skeleton) shearing along y
910	730	76	53	out-of-plane C-H bending
1030	803	54	75	C- C_d stretching + in-plane C-H, $C_d\text{-H}_d$ bending following the carbon motion
1266	985	77	66	collective in-plane C-H and $C_d\text{-H}_d$ bending (in phase)
1309	1207	47	12	in-plane C-H and $C_d\text{-H}_d$ bending (out of phase)
3064	2255	92	84	C-H stretching
<i>B₁</i> modes				
88	54	9	16	T_x of C_6H_6 + R_y of dimer (in phase)
186	181	6	12	R_y of $\text{C}_6\text{H}_6\text{-Si}_2$ with rotation axis through the adsorbate
310	299	21	15	R_y of C_6H_6 in phase with R_y of the dimer
467	438	12	26	asymmetric $\text{Si}_d\text{-C}_d$ stretching
666	589	21	49	asymmetric T_z of C and C_d (C and C_d out of phase)
871	689	43	80	C- C_d stretching + C-H bending following the carbon motions
887	740	47	49	collective out-of-plane C-H and $C_d\text{-H}_d$ bending (in phase) + skeleton shearing along x
929	917	44	25	out-of-plane C-H and $C_d\text{-H}_d$ bending (out of phase) + skeleton shearing along x
1065	834	70	30	out-of-plane $C_d\text{-H}_d$ bending
1340	1146	62	30	in-plane C-H bending
2978	2193	92	84	$C_d\text{-H}_d$ stretching
3065	2258	92	84	C-H stretching
<i>B₂</i> modes				
86	80	13	24	R_x of $\text{C}_6\text{H}_6\text{-Si}_2$ around the dimer bond
194	179	18	30	R_x of the $\text{Si}_d\text{-C}_d$ bonds around the dimer bond out of phase with R_x of C_6H_6
381	376	2	5	T_y of the dimer
678	541	74	56	out-of-plane C-H bending
945	768	35	80	C- C_d stretching + C-H, $C_d\text{-H}_d$ bending following the carbon motions
1109	788	99	97	in-plane C-H and $C_d\text{-H}_d$ bending (out of phase)
1253	1105	56	20	in-plane C-H and $C_d\text{-H}_d$ bending (in phase)
1570	1528	10	9	asymmetric C=C stretching
3079	2287	91	79	C-H stretching

“Butterfly flapping,” an internal benzene deformation with upwards and downwards bending of the sp^2 carbon atoms relative to the sp^3 centers, contributes to some extent to this stretching mode. Nevertheless, butterfly flapping is assigned to the mode at 318 cm^{-1} (exp. 315 cm^{-1}) which also features some in-phase admixture of a frustrated translation of the

whole benzene-dimer adsorption complex. With an energy in between, the dimer stretching mode is calculated at 419 cm^{-1} . This mode does not couple substantially to any other adsorbate modes; we will come back to this point in Section IV D 1. This dimer stretching mode is not discernible in the experimental spectrum which might be caused by cou-

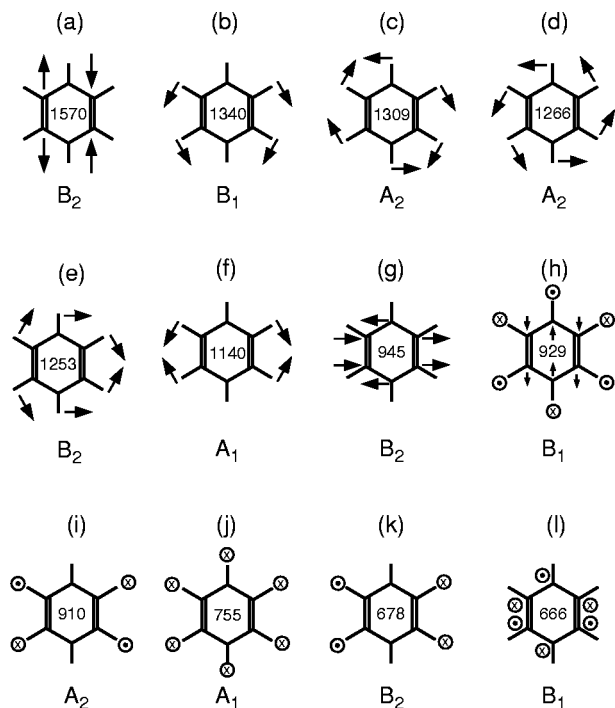


FIG. 3. Sketches of some of the calculated normal modes of the cluster model $C_6H_6Si_{13}H_{12}$. Only the benzene molecule with the remaining two $C=C$ double bonds is shown. In-plane motions of the atoms are indicated by arrows, out-of-plane motions by encircled crosses and dots (up/down).

pling to surface phonons. Two further deformation modes of the distorted carbon ring are found at 577 and 870 cm^{-1} (exp. 604 and 876 cm^{-1}), respectively. The mode at higher frequency describes ring breathing with an almost uniform in-phase variation of the benzene carbon ring diameter. The mode at 577 cm^{-1} , although similar in nature, differs by the motion of the two carbon atoms directly coordinated to the surface dimer which is opposite to that of the four sp^2 carbon centers. In comparison to the former breathing mode, this latter mode exhibits small stretching contributions of the carbon-carbon bonds only, but consists essentially of deformations of the $C-C_d-C$ angles. The corresponding force constants are significantly smaller than those of the $C-C$ stretching and thus the mode exhibits a lower frequency. The vibration at 755 cm^{-1} (exp. 776 cm^{-1}), finally, is dominated by a collective in-phase out-of-plane bending of all six benzene hydrogen atoms.

As noted previously⁵ the totally symmetric modes are sufficient to rationalize most of the prominent features of the experimental HREELS spectrum (see Fig. 2 and Table I). Except for the frustrated translation at 154 cm^{-1} , each calculated totally symmetric normal mode frequency can be assigned to an energy loss feature in the experimental spectrum, such that the average absolute deviation of the frequencies amounts to 20 cm^{-1} . The largest discrepancy (43 cm^{-1}) is found for the $C-H$ stretching modes at 2978 cm^{-1} of the $C-H$ groups directly coordinated to the surface dimer. In DF calculations deviations of vibrational frequencies of that order are not uncommon for the kind of modes discussed here.²³ The experimental spectrum also exhibits features that have to be related to nonsymmetric

modes, as will be done next. Further experimental results regarding scattering mechanisms (dipole and impact scattering), isotope shifts, coverage dependence, and step site adsorption will be presented elsewhere.¹¹

B. The nonsymmetric modes

We start the discussion of the nonsymmetric vibrational modes with the characteristic $C=C$ double bond frequency at about 1600 cm^{-1} . This energy loss, which in part can be attributed to the A_1 symmetric $C=C$ stretch (Table I), actually consists of two close lying peaks, of which the lower frequency signal is less intense; note the weak shoulder close to 1600 cm^{-1} in Fig. 2. This additional feature is due to the out-of-phase B_2 vibration of the two $C=C$ double bonds [Fig. 3(a), Table I]. The calculated frequency splitting of about 50 cm^{-1} for the two $C=C$ stretching modes, with the antisymmetric, i.e., dipole inactive mode at lower frequency (1570 cm^{-1}), is in perfect agreement with experiment.

The two energy losses at 1286 and 1378 cm^{-1} , observed experimentally, have to be attributed to in-plane $C-H$ bending modes. A total of four calculated modes exhibit appropriate frequencies, two of them of A_2 symmetry, one each of B_1 and B_2 symmetry [see Figs. 3(c,d,b,e)].

The energy loss at 949 cm^{-1} and the shoulder at about 900 cm^{-1} can be assigned to out-of-plane bending modes of the $C-H$ groups of the sp^2 carbon atoms [A_2 , B_1 modes calculated at 910 and 929 cm^{-1} , respectively; Figs. 3(i,h)] and to a stretching of the $C-C$ bonds [B_2 calculated at 945 cm^{-1} ; Fig. 3(g)]. Finally, the low intensity signal at about 700 cm^{-1} can be connected to the B_2 symmetric out-of-plane bending of the sp^2 $C-H$ groups [Fig. 3(k)] calculated at 678 cm^{-1} , and to an internal deformation mode of the benzene carbon ring with a calculated frequency of 666 cm^{-1} [see Fig. 3(l)].

Obviously there also is some structure in the experimental data between 350 and 500 cm^{-1} . Assignment of these modes is difficult because of the low intensity of these energy losses on the one hand and the large number of calculated modes with appropriate frequencies on the other hand. Nevertheless, we tentatively assign the feature at about 500 cm^{-1} to the asymmetric Si_dC_d stretching (B_1) calculated at 467 cm^{-1} and to the in-plane rotations of the $C=C$ groups around their corresponding bond centers (A_2) with a calculated frequency of 474 cm^{-1} . Three modes of the surface dimer mark the lower edge of the frequency range discussed here. Besides the A_1 symmetric dimer stretching already mentioned (419 cm^{-1}), these are the rotation of the surface dimer around the z -axis (A_2) at 402 cm^{-1} and the frustrated translation of that dimer along the dimer rows (B_2) at 381 cm^{-1} (Table I).

Thus far we have demonstrated that each experimental feature can be related to one (or several) of the calculated vibrational frequencies of the model cluster $C_6H_6Si_{13}H_{12}$. Yet, one may raise the question if there are theoretically predicted modes which are not observed in the experiment. Indeed, the number of modes resulting from the theoretical analysis by far exceeds the number of experimentally resolvable features. However, this is, at least in part, related to the fact that some of the theoretical frequencies lie close to-

gether, such that the corresponding experimental features can not be resolved unequivocally. For instance, the six C–H stretching frequencies fall into two groups with frequencies differing by less than 20 cm^{-1} . Hence, in the experimental spectra only two C–H stretching bands can be observed. In the lower frequency region, identification is even more complicated due to the profound intensity differences of impact and dipole scattered electrons in the particular experimental setup used to record the data shown in Fig. 2. Because of the much higher intensity of the dipole-active totally symmetric A_1 modes, these losses might cover up signals from vibrations of the other irreducible representations which are solely due to impact scattering. Moreover, several modes with frequencies below 300 cm^{-1} are calculated which arise from frustrated motions of the adsorbate or the entire adsorption complex. Unfortunately, an identification of these modes in the experimental spectrum is not possible so far due to their superposition with the tail of elastically scattered electrons.

Besides the few exceptions just mentioned, all theoretically predicted vibrational modes were assigned to one of the features in the experimental spectrum. This overall very good agreement of the experimental HREELS data and the calculated frequencies for the butterfly structure corroborates that benzene is indeed adsorbed in a butterfly structure on Si(001), as found in our previous combined experimental and theoretical photoemission studies of the adsorption complex.^{4,5}

C. Isotope shifts

Since frequency shifts due to deuteration strongly depend on the amount of hydrogen contribution to a normal mode, they can be used to experimentally identify the character of a normal mode. However, this kind of analysis assumes a one-to-one correspondence between the normal modes of the hydrogen species and its deuterated counterpart, i.e., the character of a normal mode should not change significantly upon deuteration. Such a one-to-one correspondence is often difficult to establish, as the original ordering of the eigenmodes may change in the deuterated species. In a theoretical approach the correlation between normal frequencies of hydrogen and their deuterated analogues can be based on a direct comparison of the modes in real space. Alternatively, the relative contribution of the hydrogen atoms to the total kinetic energy of a normal mode can be used as a criterion. In a diatomic hydride molecule with a reasonably heavy heteroatom the kinetic energy fraction x contributed by the hydrogen species is almost independent of the hydrogen isotope used, $x = m_2 / (m_1 + m_2)$ with m_2 being the mass of the heavy atom. In this sense, modes with a comparable percentage of H and D contribution to the kinetic energies can be identified with each other. The results of such an analysis of the normal modes of our models $\text{C}_6\text{H}_6\text{Si}_{13}\text{H}_{12}$ and $\text{C}_6\text{D}_6\text{Si}_{13}\text{H}_{12}$ are presented in Table I.

For most of the modes the assignment is rather straightforward. Nevertheless, there are some cases where the contribution of the deuterium to the kinetic energy of the deuterated adsorbate differs substantially from the kinetic energy fraction of the hydrogen atoms in normal benzene; e.g., the A_2 mode at 402 cm^{-1} , which is a pure rotation of the Si

dimer around the surface normal, exhibits a hydrogen contribution $E_{\text{kin}}(\text{H})$ of 3% that rises to 24% upon deuteration, indicative for a significant change in character of the normal mode. Alternatively, the hydrogen contribution of a normal mode may decrease drastically when hydrogen is substituted by deuterium. This is the case for the A_2 mode at 1309 cm^{-1} . Upon deuteration the kinetic energy fraction of the hydrogen isotopes drops from 47% to 12%. As a consequence the resulting red-shift of the frequency is rather low, $\nu(\text{C}_6\text{H}_6) / \nu(\text{C}_6\text{D}_6) = 1.08$, although the mode of the nonsubstituted benzene species, an out-of-phase C–H and $\text{C}_d\text{--H}_d$ in-plane bending accompanied by some C– C_d stretching, exhibits a substantial hydrogen contribution (47%). A similar effect is found for the B_2 mode at 1253 cm^{-1} whose kinetic energy fraction of the hydrogen atoms drops from 56% to 20% for the deuterated species. Actually, in such cases the meaning of a one-to-one correspondence becomes questionable. The isotope shifts reported here for the totally symmetric normal modes essentially coincide with those calculated and discussed previously⁵ in comparison to the experimental data available at that time.¹

The spectra of deuterated species provide important experimental data which can be used for a very detailed and thorough comparison between theory and experiment. Yet, in general, the necessity for cumbersome and laborious attempts to extract information on the real space character of individual vibrational modes from isotope shifts decreases when a reliable computed force field is available.

D. Coupling of substrate and adsorbate modes

Now, we address one of the main goals of the present study, the investigation of the vibrational coupling mechanism of benzene molecules to the Si(001) substrate. The discussion will be given in two steps. First we will focus on dynamical aspects, i.e., on the effect of the motion of substrate atoms on the vibrational spectra. Subsequently, we shall consider the influence of the Si substrate on the force constants which govern the vibrational frequencies.

1. Dynamic coupling

When analyzing adsorbate vibrations one often invokes the approximation to completely fix the positions of the substrate atoms. Certainly, this is acceptable when the substrate atoms are much heavier than the adsorbate. However, for $\text{C}_6\text{H}_6/\text{Si}(001)$ where the mass of the entire benzene molecule is even larger than that of the surface dimer, this approximation is highly questionable. Rather, the coupling between substrate and adsorbate modes strongly depends on the strength of the bonds between the surface dimer and the rest of the substrate. Two limiting cases can be considered. If the bonds between the surface dimer and the second layer silicon atoms are sufficiently strong (model I) the substrate may be regarded as rigid. In the opposite case, i.e., for extremely weak bonding between the dimer and the remaining substrate (model II), the resulting vibrations of the adsorption complex are those of a “free” benzene-dimer moiety. Of course, the actual coupling will fall somewhere between these two extremes. Thus, in the following we will examine to which

TABLE II. Comparison of calculated normal mode frequencies of the model cluster $C_6H_6Si_{13}H_{12}$ and the free “molecular” system $C_6H_6Si_2H_4$ as obtained by different vibrational analyses. The frequencies (in cm^{-1}) either refer to a full, non-constrained vibrational analysis including the motion of the surface dimer (“full”) or have been calculated according to the truncation models I, II, and II(a) (see text). Frequencies above 800 cm^{-1} have been omitted.

	$C_6H_6Si_{13}H_{12}$			$C_6H_6Si_2H_4$		
	Full	I	II	IIa	Full	IIa
A_1 modes						
154						
318		226	311	306	302	307
419				407	423	442
523		469	516	516	522	534
577		557	566	572	572	598
755		746	750	753	804	766
A_2 modes						
109		117				
402						
474		464				
608		607				
B_1 modes						
88						
186						
310			271			
467			453			
666			663			
B_2 modes						
86		86				
194		212				
381						
678		678				

extent one of the two models can serve as an approximate description for the adsorption complex at hand.

The full vibrational analysis of the adsorption complex with the motion of the dimer included will be the reference for further investigations. Since the complete force constant matrix is available it is easy to simulate the two limiting models I and II by manipulating the appropriate matrix elements.²⁴ Two variants of model II have been considered: one where the force constant associated with the dimer stretching motion is eliminated (model II) and one where this force constant is kept [model II(a)]. No significant differences were found between these two variants (see below). In the following we will refer to the special vibrational analysis described here as “truncation analysis.”

In the upper panel of Table II the totally symmetric frequencies resulting from the three different models I, II, and II(a) are compared to those of the full analysis. Significant coupling to the substrate only occurs for frequencies below 800 cm^{-1} . All other frequencies obtained by the truncation analysis differ by at most 3 cm^{-1} from the corresponding values of the full analysis, and thus are not shown in Table II. The very small frequency deviations between models II and II(a) corroborate the earlier statement that the dimer stretching does not significantly couple with any other totally symmetric mode (Table I). However, most amazing in the present context is the very good agreement over the entire frequency range between the frequencies of the full analysis and those of models II and II(a). This suggests that the sur-

face dimer moves almost freely relative to the rest of the substrate.

The reason for this result can be found in the ratios of the involved force constants and masses. To demonstrate this we will refer to a simple two-mode (TM) coupling model of the adsorption complex²⁴ which comprises only the two most important degrees of freedom: the frustrated motion of the entire $C_6H_6-Si_2$ moiety with respect to the remaining substrate and the collective motion of the adsorbate against the Si surface dimer. This TM coupling model is formally equivalent to a system of two masses and a rigid wall which are connected to each other by springs; it admits a detailed analysis of the vibrational patterns.²⁴ Of course, it also encompasses the two limiting cases, model I and model II. Based on analytical expressions²⁴ that depend solely on the ratio of the force constants and masses involved, one can decide (after fixing a threshold) whether a system belongs to one of the two limiting cases or not.

Actually, not only for the totally symmetric modes, but for each irreducible representation there exists (at least) one frustrated motion of the entire adsorption complex $C_6H_6-Si_2$ and a corresponding intracomplex vibrational mode which can be regarded as a realization of the TM model.²⁴ While motions of A_1 , A_2 , and B_2 symmetry permit only one such realization, there are two for the B_1 representation: one based on the translational degrees of freedom, $B_1(\text{trans})$, the other one based on the rotational degrees of freedom, $B_1(\text{rot})$.

According to the calculated force constants quite different vibrational patterns occur depending on the symmetry of the vibrations considered. The A_1 and $B_1(\text{rot})$ motions of the adsorption system represent model II, the regime of weak dimer–substrate coupling with an essentially isolated adsorption complex $C_6H_6-Si_2$. For the A_2 and B_2 motions the situation is opposite: the adsorption system exhibits strong dimer–substrate coupling (model I) where the benzene molecule can essentially be regarded as bound to a rigid substrate surface. The $B_1(\text{trans})$ realization, finally, falls into an intermediate regime where no simple characterization of the vibrational pattern is possible.²⁴

This classification is corroborated by the force constant truncation technique. Applying this method to the nonsymmetric vibrational modes of the adsorption complex yields the frequencies summarized in the lower part of Table II. As for the totally symmetric modes, the details of the treatment of the surface dimer does not influence vibrational modes above 800 cm^{-1} . Based on the classification proposed above, the truncation analysis is performed according to model I for the A_2 and B_2 representations and according to model II for the B_1 representation. The agreement between the frequencies of the model cluster $C_6H_6Si_{13}H_{12}$ and those of the appropriately truncated models is remarkable (Table II) confirming the characterization of the soft vibrational modes of the adsorption system $C_6H_6/Si(001)$ based on the simplified two-mode coupling model.

A nice geometrical rationalization may be given for this classification. Within the representations A_2 and B_2 the Si atoms of the surface dimer are restricted to move in a plane parallel to the surface. These motions are essentially associated with a stretching of the relatively stiff covalent Si–Si

TABLE III. Comparison of structural parameters calculated for the model cluster $C_6H_6Si_{13}H_{12}$ and a free “molecular” system $C_6H_6Si_2H_4$. For the labeling of the atoms see Fig. 1. Bond length in Å, bond angles in degrees.

Quantity	$C_6H_6Si_{13}H_{12}$	$C_6H_6Si_2H_4$
$d(CC)$	1.350	1.348
$d(CC_d)$	1.510	1.514
$\angle(HCC)$	121.6	122.0
$\angle(HCC_d)$	119.3	119.4
$\angle(CCC_d)$	119.1	118.6
$\angle(CC_dC)$	110.1	110.1
$\angle(H_dC_dC)$	112.8	112.6
$d(Si_dC_d)$	1.967	1.944
$\angle(CC_dSi_d)$	104.8	104.8
$\angle(C_dSi_dSi_d)$	95.4	96.6
$\angle(C_dSi_dSi)$	118.5	
$d(Si_dSi_d)$	2.448	2.351
$d(Si_dSi)$	2.370	

bonds between the surface dimer and the first subsurface Si atoms. For the A_1 and B_1 representations the elongation of the surface dimer Si is restricted to the vertical symmetry plane containing the dimer axis. Stretching of bonds to the substrate is much less important for these motions; rather the corresponding bond angles are deformed. Similar observations hold for the adsorbate motion. Within the A_1 and $B_1(\text{rot})$ realizations, Si_d-C_d bond stretching is important whereas for the other three realizations, A_2 , B_2 , and $B_1(\text{trans})$ bending deformations of the Si_2C_2 ring of the adsorption complex represent the main character of the vibrational modes involved. This analysis suggests a somewhat stronger adsorbate–dimer coupling compared to the dimer–substrate coupling in case of the A_1 and $B_1(\text{rot})$ realizations (model I), and vice versa a much weaker adsorbate–dimer coupling with respect to the dimer–substrate coupling for the A_2 and B_2 representations (model II). Finally, realization $B_1(\text{trans})$ falls into the intermediate regime because here, in contrast to the $B_1(\text{rot})$ realization, no significant Si–C stretching is involved in the characteristic motion of this realization.

2. Electronic coupling

After the analysis of the dynamical aspects of the adsorbate–surface coupling we now investigate to which extent the embedding into a Si surrounding influences the force constants and accordingly the frequencies of the $C_6H_6-Si_2$ moiety. To this end, we study the molecular system $C_6H_6Si_2H_4$, a minimal model for the adsorption complex in absence of any surrounding substrate. The optimized geometry of this system very much resembles that of the cluster $C_6H_6Si_{13}H_{12}$ (see Table III). The differences in the internal benzene coordinates amount to a few thousands of an Å or several tenths of a degree only. The largest discrepancy occurs for the Si–Si bond length which is by about 0.1 Å shorter in the “molecule” than in the adsorption model $C_6H_6Si_{13}H_{12}$. This is related to the missing stress which acts on the real adsorption complex. Likewise, the calculated totally symmetric normal modes of $C_6H_6Si_2H_4$ and their frequencies (Table II) show great similarity with the corre-

sponding quantities of the chemisorption model cluster $C_6H_6Si_{13}H_{12}$. Omission of all degrees of freedom related to the hydrogen atoms which saturate the dimer bonds corresponds to a truncation analysis of $C_6H_6Si_2H_4$ according to model II(a) (see Table II). For frequencies above 800 cm^{-1} (not shown) the truncated vibrational analyses of the model cluster $C_6H_6Si_{13}H_{12}$ and the molecule $C_6H_6Si_2H_4$ exhibit even better agreement (with deviations below 10 cm^{-1}) than the full vibrational analysis of these two moieties. For the lower frequencies the impact of removing the substrate is larger as direct bonds between the adsorbate and the substrate are involved. The largest influence, a shift by 35 cm^{-1} , is found for the stretching mode of the surface dimer (at 407 cm^{-1}). Also affected are the Si_d-C_d stretching mode at 516 cm^{-1} (a 18 cm^{-1} shift) and the C– C_d –C bending mode at 572 cm^{-1} (a 26 cm^{-1} shift).

Nevertheless, the above comparison between the free molecule $C_6H_6Si_2H_4$ and the surface model cluster $C_6H_6Si_{13}H_{12}$ indicates that the geometrical and vibrational structure of the adsorption complex $C_6H_6/Si(001)$ is mainly determined by the interactions internal to the adsorption complex, at least as far as the totally symmetric vibrational modes are concerned. Obviously, the presence of the surrounding silicon substrate is of minor importance here, confirming once again that the totally symmetric motion of the adsorption complex $C_6H_6/Si(001)$ can be described as free relative to the substrate.

V. SUMMARY

In this work the vibrational properties of benzene adsorbed on Si(001) have been studied in detail. New HREELS data for the saturated monolayer as well as new density functional model cluster calculations have been presented. Experimentally, 16 benzene-derived modes with frequencies above 200 cm^{-1} have been found. Using the surface model cluster $C_6H_6Si_{13}H_{12}$ all vibrational frequencies of the adsorption complex $C_6H_6/Si(001)$ including the surface dimer motion have been calculated. All totally symmetric, dipole active modes for frequencies above 200 cm^{-1} have been assigned. Modes excited by impact scattering were rationalized with the aid of nonsymmetric vibrational modes. The discrepancy between the measured and calculated frequencies averages to 20 cm^{-1} , with maximum deviations of 43 cm^{-1} . This agreement between experiment and theory is regarded as further evidence for the butterfly (cyclohexadiene-like) adsorption geometry of $C_6H_6/Si(001)$ as assigned previously in our combined experimental and theoretical studies.^{4,5}

The vibrational coupling between the adsorbate and the substrate has been studied with the help of a truncated frequency analysis where certain adsorbate–substrate entries in the force constant matrix are eliminated. The results could be rationalized by means of a simplified two-dimensional coupling model which only takes into account the most important motions of the adsorption complex. Depending on the symmetry of the normal modes, quite different coupling mechanisms were found for the collective modes. For the A_1 and B_1 modes the idealized picture of a benzene molecule strongly bound to the surface dimer below is most appropri-

ate; the resulting moiety $C_6H_6-Si_2$ is only relatively weakly bound to the rest of the substrate. In contrast, in the A_2 and B_2 modes, the connection between the surface dimer and the surrounding silicon substrate is rather strong; here the idealization of a benzene molecule bound to a rigid surface is better suited. Thus for a consistent treatment of low-frequency modes of all irreducible representations the surface dimer directly involved in the formation of the adsorbate–substrate bond has to be included in the frequency analysis.

Comparison of the calculated totally symmetric vibrational spectra of the model cluster $C_6H_6Si_{13}H_{12}$ with those obtained for the (free) molecular system $C_6H_6Si_2H_4$ revealed that the influence of the Si surrounding on the structure of the adsorption complex and on the force constants of the benzene dimer moiety is relatively weak. In view of all these findings, we expect that a vibrational analysis of benzene adsorbed on Si(001) based on larger surface model clusters will yield essentially the same results as the present study of the model $C_6H_6Si_{13}H_{12}$.

ACKNOWLEDGMENTS

We thank Professor. J. Sauer for stimulating discussions. This work was supported by the Deutsche Forschungsgemeinschaft via SFB 338 and the Fonds der Chemischen Industrie.

¹Y. Taguchi, M. Fujisawa, T. Takaoka, T. Okada, and M. Nishijima, *J. Chem. Phys.* **95**, 6870 (1991).

²B. I. Craig, *Surf. Sci.* **280**, L279 (1993).

³H. D. Jeong, S. Ryu, Y. S. Lee, and S. Kim, *Surf. Sci.* **344**, L1226 (1995).

⁴S. Gokhale, P. Trischberger, D. Menzel, W. Widdra, H. Dröge, H.-P.

Steinrück, U. Birkenheuer, U. Gutdeutsch, and N. Rösch, *J. Chem. Phys.* **108**, 5554 (1998).

⁵U. Birkenheuer, U. Gutdeutsch, and N. Rösch, *Surf. Sci.* **409**, 213 (1998).

⁶B. Borovsky, M. Krueger, and E. Ganz, *Phys. Rev. B* **57**, R4269 (1998).

⁷G. P. Lopinski, D. J. Moffatt, and R. A. Wolkow, *Chem. Phys. Lett.* **282**, 305 (1998).

⁸G. P. Lopinski, T. M. Fortier, D. J. Moffatt, and R. A. Wolkow, *J. Vac. Sci. Technol. A* **16**, 1037 (1998).

⁹K. W. Self, R. I. Pelzel, J. H. G. Owen, C. Yan, W. Widdra, and W. H. Weinberg, *J. Vac. Sci. Technol. A* **16**, 1031 (1998).

¹⁰M. Staufer, U. Birkenheuer, and N. Rösch (unpublished).

¹¹B. Naydenov, K. L. Kostov, D. Menzel, and W. Widdra (in preparation).

¹²K. L. Kostov, M. Gsell, P. Jakob, T. Moritz, W. Widdra, and D. Menzel, *Surf. Sci.* **394**, L138 (1997).

¹³PARAGAUS 1.9, T. Belling, T. Grauschopf, S. Krüger, F. Nörtemann, M. Staufer, M. Mayer, V. A. Nasluzov, U. Birkenheuer, and N. Rösch, Technische Universität München, 1998.

¹⁴T. Belling, T. Grauschopf, S. Krüger, M. Mayer, F. Nörtemann, M. Staufer, C. Zenger, and N. Rösch, in *High Performance Scientific and Engineering Computing, Proceedings of the International FORTWHIR Conference on HPSEC*, edited by H.-J. Bungartz, F. Durst, and C. Zenger, Lecture Notes in Computational Science and Engineering (Springer, Heidelberg, 1999), Vol. 8, p. 439.

¹⁵B. I. Dunlap and N. Rösch, *Adv. Quantum Chem.* **21**, 317 (1990).

¹⁶N. Rösch, in *Cluster models for Surface and Bulk Phenomena*, edited by G. Pacchioni, P. S. Bagus, and F. Parmigiani, NATO ASI Ser. B (Plenum, New York, 1992), p. 251.

¹⁷J. A. Pople, P. M. W. Gill, and B. G. Johnson, *Chem. Phys. Lett.* **199**, 557 (1992).

¹⁸P. M. W. Gill, B. G. Johnson, and J. A. Pople, *Chem. Phys. Lett.* **209**, 506 (1993).

¹⁹S. H. Vosko, L. Wilk, and M. Nusair, *Can. J. Phys.* **58**, 1200 (1980).

²⁰A. Becke, *Phys. Rev. A* **38**, 3098 (1988).

²¹J. P. Perdew, *Phys. Rev. B* **33**, 8822 (1986).

²²J. P. Perdew, *Phys. Rev. B* **34**, 7406 (1986).

²³A. Görling, S. B. Trickey, P. Gisdakis, and N. Rösch, in *Topics in Organometallic Chemistry*, J. Brown and P. Hofmann (Springer, Heidelberg, 1999), Vol. 4, p. 109.

²⁴U. Birkenheuer and M. Staufer (in preparation).